Available online at www.sciencedirect.com
SCIENCE DIRECT®
Nuclear Instruments and Methods in Physics Research B 242 (2006) 523–529
NIM B
Beam Interactions with Materials & Atoms
www.elsevier.com/locate/nimb

Anisotropic deformation of metallo-dielectric core–shell colloids under MeV ion irradiation

J.J. Penninkhof [a,*], T. van Dillen [a,1], S. Roorda [a,b], C. Graf [c,2], A. van Blaaderen [c], A.M. Vredenberg [c], A. Polman [a]

[a] FOM Institute for Atomic and Molecular Physics, Kruislaan 407, NL-1098 SJ Amsterdam, The Netherlands
[b] Département de Physique, Université de Montreal, P.O. Box 6128, Montreal, Que., Canada H3C3J7
[c] Debye Institute, Utrecht University, Princetonplein 5, NL-3584 CC Utrecht, The Netherlands

Available online 23 September 2005

Abstract

We have studied the deformation of metallo-dielectric core–shell colloids under 4 MeV Xe, 6 and 16 MeV Au, 30 MeV Si and 30 MeV Cu ion irradiation. Colloids of silica surrounded by a gold shell, with a typical diameter of 400 nm, show anisotropic plastic deformation under MeV ion irradiation, with the metal flowing conform the anisotropically deforming silica core. The 20 nm thick metal shell imposes a mechanical constraint on the deforming silica core, reducing the net deformation strain rate compared to that of pure silica. In colloids consisting of a Au core and a silica shell, the silica expands perpendicular to the ion beam, while the metal core shows a large elongation along the ion beam direction, provided the silica shell is thick enough (>40 nm). A minimum electronic energy loss of 3.3 keV/nm is required for shape transformation of the metal core. Silver cores embedded in a silica shell show no elongation, but rather disintegrate. Also in planar SiO_2 films, Au and Ag colloids show entirely different behavior under MeV irradiation. We conclude that the deformation model of core–shell colloids must include ion-induced particle disintegration in combination with thermodynamical effects, possibly in combination with mechanical effects driven by stresses around the ion tracks.

PACS: 61.43.Fs; 61.80.Az; 61.80.Jh; 61.82.Ms; 62.20.Fe; 68.37.Hk; 82.70.Dd

Keywords: Anisotropic deformation; Ion irradiation; Colloid; SiO_2; Au; Ag; Thermal spike

1. Introduction

Amorphous materials subject to MeV ion irradiation can undergo anisotropic plastic deformation at constant volume [1]. The deformation is well described by a viscoelastic model, in which the thermal expansion of the cylindrically shaped high-temperature ion track region causes shear stresses that relax by viscous flow, with the viscous strains subsequently frozen in upon rapid cooling of the ion track region [2,3]. The deformation is induced by electronic energy loss, and thus occurs most efficiently with ions in the MeV energy range.

One of the most striking examples of this effect is the deformation of colloidal particles under MeV ion irradiation [4,5]. Spherical silica colloids expand perpendicular to the ion beam and contract parallel to the ion beam changing their shape to oblate ellipsoidal. This is illustrated in Fig. 1(a) which shows a scanning electron microscopy (SEM) image of a 1-μm-diameter silica colloid before (left) and after (right) 16 MeV Au irradiation at 77 K to a fluence of 1.1×10^{15} cm^{-2}. A shape anisotropy with a size aspect ratio (major-to-minor axis) as large as five is observed at this fluence. This ion beam deformation

* Corresponding author. Tel.: +31 20 6081234; fax: +31 20 6684106.
E-mail address: penninkhof@amolf.nl (J.J. Penninkhof).
[1] Present address: Department of Applied Physics, University of Groningen, Nijenborgh 4, NL-9747 AG Groningen, The Netherlands.
[2] Present address: Institut für Physikalische Chemie, Universität Würzburg, Am Hubland, D-97074 Würzburg, Germany.

0168-583X/$ - see front matter © 2005 Elsevier B.V. All rights reserved.
doi:10.1016/j.nimb.2005.08.116

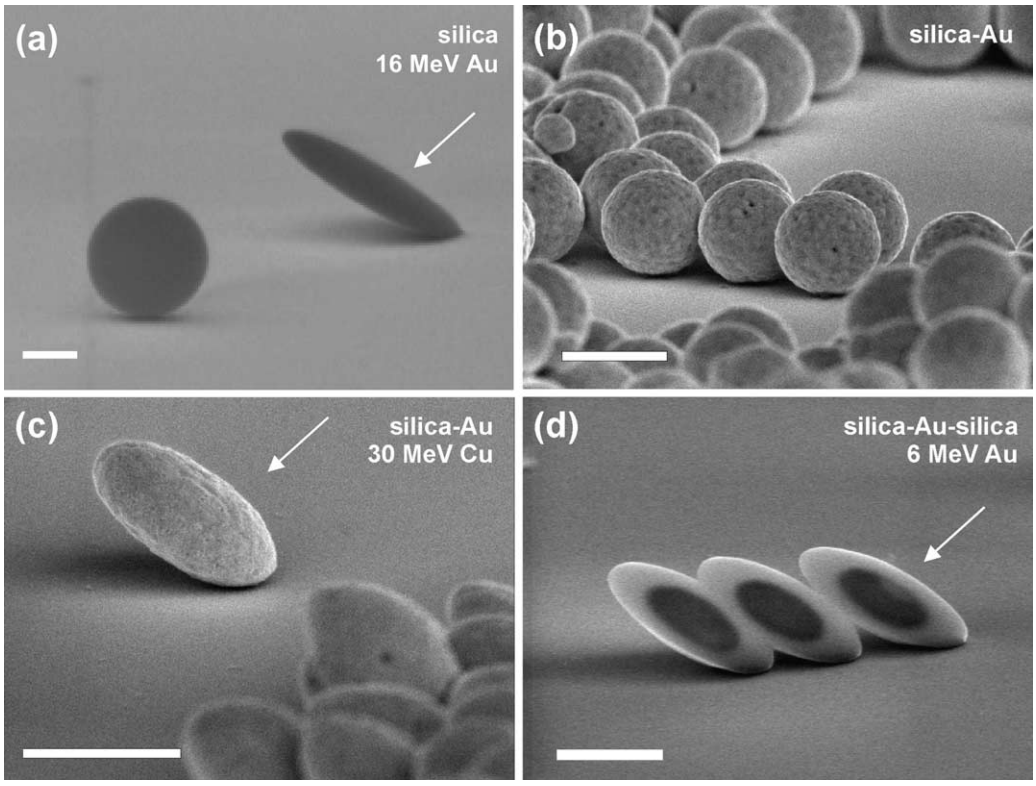

Fig. 1. SEM images of (a) silica colloid ($d = 1$ μm) before (left) and after (right) 16 MeV Au irradiation (1.1×10^{15} cm^{-2}); (b) silica–Au core–shell colloid ($d_{SiO_2} = 438$ nm, $t_{Au} = 46$ nm); (c) same as (b), after 30 MeV Cu irradiation (5×10^{14} cm^{-2}); (d) silica–Au–silica core–shell–shell colloid ($d_{SiO_2} = 300$ nm, $t_{Au} = 25$ nm, $t_{SiO_2} = 133$ nm) after 6 MeV Au irradiation (6.5×10^{14} cm^{-2}). Scale bars 500 nm.

technique provides a unique method to tailor the shape of colloidal particles and aggregates. For example, prolate ellipsoids can be made by using subsequent ion irradiations from different directions [4]. Also, the optical properties of three-dimensional colloidal photonic crystals can be tailored by ion beam deformation [6]. And recently, we demonstrated how a colloidal mask for nanolithography can be modified by MeV ion irradiation [7].

In general, amorphous materials (insulators, semiconductors or metallic glasses) show anisotropic deformation under MeV ion irradiation [8–10]. In contrast, pure metals do not show anisotropic deformation [1,11]. This is attributed to the fact that epitaxial recrystallization at the solid–liquid ion track interface would restore the initial crystalline state, without anisotropic deformation. It has also been suggested that the ion track temperature in crystalline metals does not exceed the melting temperature as a result of rapid redistribution of the deposited energy in the electronic subsystem [12].

Given the entirely different behavior of metals and silica glass under MeV ion irradiation, it is interesting to study the deformation effect on assemblies in which silica and metal are in intimate contact. In this paper we study the ion irradiation-induced deformation of colloidal particles composed of a silica core covered by a Au shell, named hereafter silica–Au core–shell colloids, and the reverse structure, a metal core with a silica shell, named (Au, Ag)–silica core–shell colloids. We show that, while single Au colloids do not show deformation, the presence of a silica core or shell induces a shape change on the metal of which the nature depends on the core–shell geometry. We compare these data for freestanding core–shell colloids with the deformation of Au and Ag colloids that are embedded in a bulk SiO_2 film and with recent work by D'Orléans et al. on Co colloids in SiO_2 films [13–16].

The motivation for this work is twofold. First, metallo-dielectric colloids form a new class of interesting building blocks for photonic applications that critically depend on the particle shape. Ion irradiation-induced deformation provides a unique tool to tailor the optical properties. Second, studies of metallo-dielectric composites could provide information on fundamental aspects of ion–solid interactions in both silica and metal. This paper focuses on the latter.

2. Experimental

Silica–Au core–shell colloids were synthesized using the method described in [17]. In brief, monodisperse silica colloids with diameters in the range between 300 nm and 500 nm were synthesized using the Stöber growth method [18], and functionalized with 3-amino-propyl-trimethoxysilane to enable the attachment of small gold nanoclusters (1–2 nm in diameter). The Au shell was grown via reduction of an aged solution of chloroauric acid by addition of a hydroxylamine hydrochloride solution. The thickness

of the Au shell was controlled by the ratio of the amount of precursor particles and the volume of the gold salt solution. Thicker Au shells were grown by seeded growth.

Au–silica core–shell colloids were grown using Au colloids with a diameter of 14 nm as a starting point. These colloids were synthesized via the standard sodium citrate reduction method. A silica shell was then grown via functionalization of the Au particles by polyvinylpyrrolidone [19], after which the colloids were transferred into ethanol to enable Stöber growth of the silica shell. Using a similar process, some silica–Au core–shell colloids were coated with an additional silica shell, leading to the formation of silica–Au–silica core–shell–shell particles. After synthesis, a droplet of the colloidal suspensions was dried on a Si(1 0 0) substrate under nitrogen flow, so that the typical surface coverage was well below a monolayer. For transmission electron microscopy (TEM) analysis, colloids were deposited on a 10-nm thick Si_3N_4 membrane embedded in a Si wafer.

Au and Ag colloids were also synthesized in planar SiO_2 films, made by thermal oxidation of a Si substrate. Multiple-energy Au and Ag implants were used with energies in the range 45–200 keV to yield constant Ag or Au depth profiles at a concentration of 1.6×10^{21} cm^{-3}. Spherical colloids were then formed in SiO_2 by thermal annealing at 500 °C (Ag) or 1150 °C (Au).

Ion irradiation was performed using Van de Graaff tandem accelerators in Utrecht, Montreal and Rossendorf. The samples were mounted onto a copper substrate holder that was cooled to 77 K using liquid nitrogen, since largest anisotropic deformation is observed at low temperatures [20,21]. The ion beam was electrostatically scanned across an area of typically a few cm^2. Electron microscopy (SEM: 5–30 keV and TEM: 120–200 keV) was used to determine the particles' size and shape before and after ion irradiation.

3. Results and discussion

3.1. Silica–Au core–shell colloids

A side-view SEM image (10° tilt angle with respect to the substrate surface) of silica–Au core–shell colloids on a Si substrate is shown in Fig. 1(b). The silica core diameter is 438 nm and the Au shell thickness is 46 nm. Fig. 1(c) shows the sample after irradiation with 30 MeV Cu ions to a fluence of 5×10^{14} cm^{-2} at 45°. The colloids are imaged almost perpendicular to the ion beam direction, at a side-view tilt angle of 10°. Clearly, the colloids have expanded perpendicular to the ion beam and contracted parallel to the ion beam. The silica core remains uniformly covered with Au after the deformation and the size aspect ratio is 1.47 ± 0.16.

Fig. 1(c) clearly shows how the deformation of the silica core imposes a deformation on the Au shell that would otherwise not deform under irradiation. The conformal shape transformation of the metal is attributed to radiation-induced viscous flow that leads to an effective softening of the metal under irradiation. Indeed, metals such as Al and W are known to relax stress by ion irradiation-induced Newtonian viscous flow [22,23].[3] This is further supported by the observation in Fig. 1(c) that the metal shell surface appears somewhat smoothened after irradiation. The aspect ratio observed in Fig. 1(c) is 60% smaller than that observed for pure silica colloids (without Au shell), suggesting that the presence of the metal imposes a mechanical constraint on the deforming silica core [24]. Extrapolation of experiments on colloids with different Au shell thicknesses, presented elsewhere [25], show that when the Au shell thickness exceeds 100 nm, the deformation of the silica core is almost fully suppressed. The data in this section are all consistent with a continuum mechanical model, with the final deformation of the core–shell colloid determined by the ion beam-induced anisotropic deformation strain in the silica, and the radiation-induced viscosities in both silica and metal.

Fig. 1(d) shows an SEM image of a 300-nm diameter silica colloid covered with a 25-nm thick Au shell and an additional 133-nm thick silica shell. The colloids were irradiated with 6 MeV Au ions to a fluence of 6.5×10^{14} cm^{-2} at an angle of 45° at 77 K. In the SEM image, taken using a 30 keV electron beam, the embedded (deformed) Au shell appears as a clear contrast. The size aspect ratio of these silica–Au–silica core–shell–shell colloids is 2.86 ± 0.11. Comparing the particle anisotropy with that of a silica–Au colloid under the same irradiation conditions (size aspect ratio 1.69 ± 0.19), it appears that the additional silica shell increases the overall deformation. When the silica shell thickness is increased, the overall deformation approaches that of pure silica colloids of equal size (data not shown).

We have also performed experiments on the deformation of silica cores covered with a silver shell. Very similar deformation effects are observed as for the Au shell, with the Ag flowing conform with the silica core's shape, leading to the formation of an anisotropic Ag shell.

3.2. Au–silica core–shell colloids

Fig. 2(a) shows a TEM image of a spherically shaped Au–silica core–shell particle with a Au core diameter of 14 nm and a silica shell thickness of 75 nm. A TEM image of a collection of these colloids after irradiation with 30 MeV Cu ions (1×10^{15} cm^{-2}) is shown in Fig. 2(b). The ion beam direction is schematically indicated. Clearly, during irradiation the silica shell has turned into the expected oblate ellipsoidal shape. The Au core however, has deformed in an entirely different manner: it is effectively elongated along the ion beam and narrowed perpendicular to the beam [26]. The typical length of the Au rods

[3] Note that the latter is an effect of entirely different nature that the anisotropic strain generation that leads to plastic deformation of the silica (see [30]).

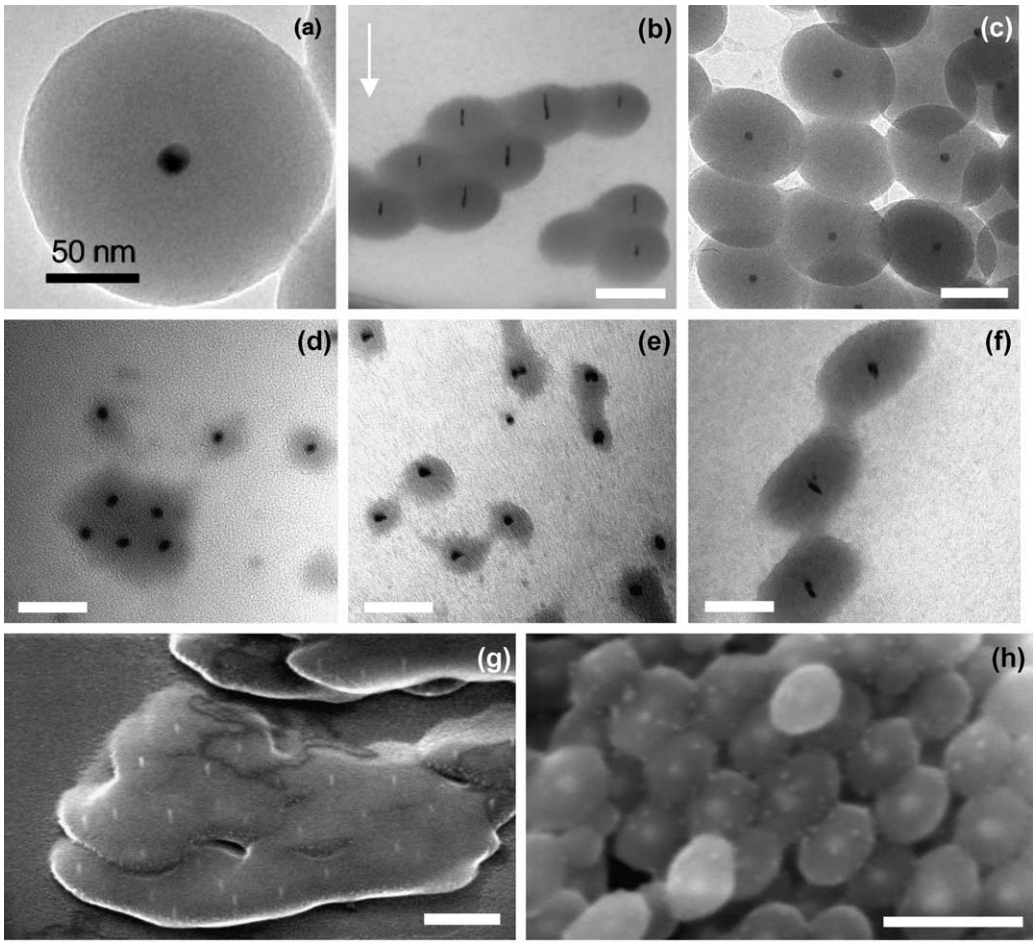

Fig. 2. TEM (a–f) and SEM (g–h) images of (a) Au–silica core–shell colloid ($d_{Au} = 14$ nm, $t_{SiO_2} = 72$ nm); (b) Au–silica core–shell colloid ($d_{Au} = 14$ nm, $t_{SiO_2} = 65$ nm) after 30 MeV Cu irradiation (1×10^{15} cm^{-2}); (c) Au–silica core–shell colloid ($d_{Au} = 15$ nm, $t_{SiO_2} = 72$ nm) after 4 MeV Xe irradiation (4×10^{14} cm^{-2}); (d)–(f) Au–silica core–shell colloids ($d_{Au} = 14$ nm, $t_{SiO_2} = 26$ nm (d), 39 nm (e), 72 nm (f)) after 30 MeV Cu irradiation (2×10^{14} cm^{-2}); (g) Au–silica core–shell colloids ($d_{Au} = 15$ nm, $t_{SiO_2} = 65$ nm) after 30 MeV Cu irradiation (2×10^{15} cm^{-2}); (h) Ag–silica core–shell colloids ($d_{Ag} = 26$ nm, $t_{SiO_2} = 47$ nm) after 30 MeV Si irradiation (4.7×10^{14} cm^{-2}). Scale bars 50 nm (a), 100 nm (b–f) or 200 nm (g, h).

observed in the image is 35–50 nm. Assuming volume conservation this translates into a size aspect ratio of ~6.

This intriguing deformation effect was studied further by irradiations with other ions than Cu. Fig. 2(c) shows a TEM image of core–shell colloids (Au diameter $d_{Au} =$ 15 nm, silica shell thickness $t_{SiO_2} = 65$ nm) after irradiation with 4×10^{14} Xe/cm^2. Again, clear deformation of the silica shell is observed, but no measurable shape change of the Au core is found. This indicates that the deformation mechanisms of metal core and silica shell are not directly related. Additional experiments using 30 MeV Si ions also showed no deformation of the Au core. In Table 1 the electronic and nuclear energy losses for 4 MeV Xe, 6 MeV Au, 30 MeV Si, and 30 MeV Cu ions are listed for irradiations in silica, Ag and Au [27]. Comparing these numbers, we find an electronic energy loss threshold (in the silica) for deformation of the Au core of $S_e^{th} > 3.3$ keV/nm. Note that, as we have shown earlier, anisotropic deformation of (colloidal) silica shows no measurable threshold ($S_e^{th} < 0.4$ keV/nm) [21].

To study this in more detail, a series of core–shell particles was made with different silica shell thicknesses.

Table 1
Overview of electronic and nuclear energy losses S_e and S_n in keV/nm for 4 MeV Xe, 6 MeV Au, 30 MeV Si and 30 MeV Cu ions in silica (density 2.0 g/cm^3), gold and silver

	4 MeV Xe		6 MeV Au		30 MeV Si		30 MeV Cu	
	S_e	S_n	S_e	S_n	S_e	S_n	S_e	S_n
Silica	1.50	0.79	2.47	1.41	3.34	0.005	5.85	0.04
Au	2.64	3.39	4.82	6.44	10.5	0.02	16.8	0.18
Ag	2.80	2.53	4.65	4.70	8.6	0.02	14.4	0.13

Fig. 2(d)–(f) shows TEM images of particles with a 14-nm thick Au core, embedded in silica shells with a thickness of about 30 nm (d), 40 nm (e), or 70 nm (f) after 30 MeV Cu irradiation. For the latter shell thickness a clear elongation of the Au cores is observed.[4] This indicates that the deformation of the metal core is somehow related to ion-induced effects in the silica shell. An additional observation of similar nature, published in [26], is that for core–shell particles of equal size and shell thickness the deformation of the metal core depends on the local surroundings of the particles: particles that are stacked two or three layers thick and are in contact before irradiation exhibit significantly larger deformation of the metal core than isolated particles. From these two independent experiments (varying shell thickness and varying colloid contact) we conclude that the Au core deforms more efficiently when more silica surrounds it.

Fig. 2(g) shows an SEM image of a two-dimensional array of Au–silica core–shell particles ($d_{Au} = 15$ nm, $t_{SiO_2} = 65$ nm) that was irradiated with 30 MeV Cu (2×10^{15} cm^{-2}). Clearly, at this high fluence the silica shows large deformation, and the colloids have completely flown together. The Au cores, however, again show a clear elongation along the ion beam, leading to the formation of a regular array of aligned Au nanorods with lengths as long as 30 nm.

Next, we study the irradiation of core–shell colloids composed of a silver core and a silica shell. Fig. 2(h) shows an SEM image of a Ag–silica core–shell colloid ($d_{Ag} = 26$ nm, $t_{silica} = 47$ nm) after 30 MeV Si irradiation to a fluence of 4.7×10^{14} cm^{-2}. An entirely different effect is observed for Ag than for the Au cores described above: the Ag cores have disintegrated and reassembled in small nanoparticles that seem to preferentially form at the colloid's surface. The difference between the ion irradiation effects on Au and Ag cores is striking and provides a hint that the mechanism for elongation of the metallic cores may include effects of melting and vaporization of the metal, as well as diffusivity and solubility of the metal in the glass matrix.

Disintegration of small Co clusters (radius smaller than 6–8 nm) and anisotropic deformation of larger Co clusters in silica was also observed by D'Orléans et al. for 200 MeV I irradiations [13]. The effects are ascribed to the fragmentation or deformation creep of the clusters in the thermal spike region. In another study, Heinig et al. [28] also observed disintegration of nanoparticles under ion irradiation. They attributed this to an "inverse Ostwald ripening process" that can occur under particular conditions of ion irradiation kinetics and thermodynamics. The ion beam-induced disintegration of the Ag cores is then related to the large solubility and particular bonding nature of Ag in the silica network. Moreover, Bernas et al. [29], have found that ion irradiation-induced nucleation and growth of Ag nanoparticles in silica glass has a strong thermodynamically driven component.

One model that we have proposed earlier to explain the elongation of the Au core is an indirect deformation scenario in which the in-plane strain generated by ion tracks in the silica shell imposes a stress on the metal core [26]. With the metals being relatively soft under ion irradiation (see the shape change of metal shells in Section 3.1) this in-plane stress may then cause the metal core to flow in the out-of-plane direction, i.e. along the direction of the ion beam, by Newtonian viscous flow. This argument seems consistent with the fact that larger elongation is found for colloids with a thicker silica shell, or for colloidal assemblies that are more closely packed [26]. The fact that entirely different electronic stopping thresholds are found for elongation of the Au core ($S_e^{th} > 3.3$ keV/nm) and the deformation of the silica shell ($S_e^{th} < 0.4$ keV/nm) implies that this indirect deformation model is too simple, unless a radiation-induced Newtonian flow mechanism is invoked in which the metal would only flow above a particular threshold electronic energy loss. However, we have shown previously that radiation-induced viscous flow is an effect that is determined by energy deposition in atomic displacements, rather than electronic excitations [30]. It would thus be less efficient for 30 MeV Cu irradiation than for 4 MeV Xe or 30 MeV Si irradiation, contrary to what is observed. This implies that the indirect deformation scenario does not seem consistent with the data. Most likely, ion-induced particle disintegration in combination with thermodynamical effects play a role, possibly in combination with mechanical effects driven by stresses around the ion tracks. Recent experiments by Vredenberg et al. on the deformation of colloidal Au particles embedded in planar SiO_2 films will shed further light on this issue [31].

3.3. Au and Ag colloids in planar SiO_2 films

To further study the different behavior of Au and Ag, we prepared Au and Ag colloids in planar SiO_2 films, using ion implantation and thermal annealing. Fig. 3(a) and (c) shows cross-section TEM images of the Au and Ag doped layers after implantation and thermal annealing. The Au implanted sample shows Au colloids arranged in two bands, centered at depths of 80 nm and 100 nm, with typical colloid diameters of 5–20 nm. The Ag implanted sample shows a large density of much smaller colloids.

After irradiation with 30 MeV Si (9.3×10^{14} cm^{-2}) at an angle of 60° relative to the surface normal, clear deformation of the Au colloids is observed (Fig. 3(b)). Similar to what is observed for the Au–silica core–shell colloids (Fig. 2(b), (f) and (g)), the Au elongates along the ion beam. A typical size aspect ratio of 2 is observed. Fig. 3(d) shows the Ag doped sample after irradiation under the same conditions. No deformation of the Ag colloids is observed. This again indicates that thermodynamical effects are likely to play a role in the deformation mechanism.

[4] Note that in Fig. 2(f) not all elongated Au cores seem aligned in the same direction. This is attributed to the fact that the TEM grid has wrinkled somewhat during irradiation.

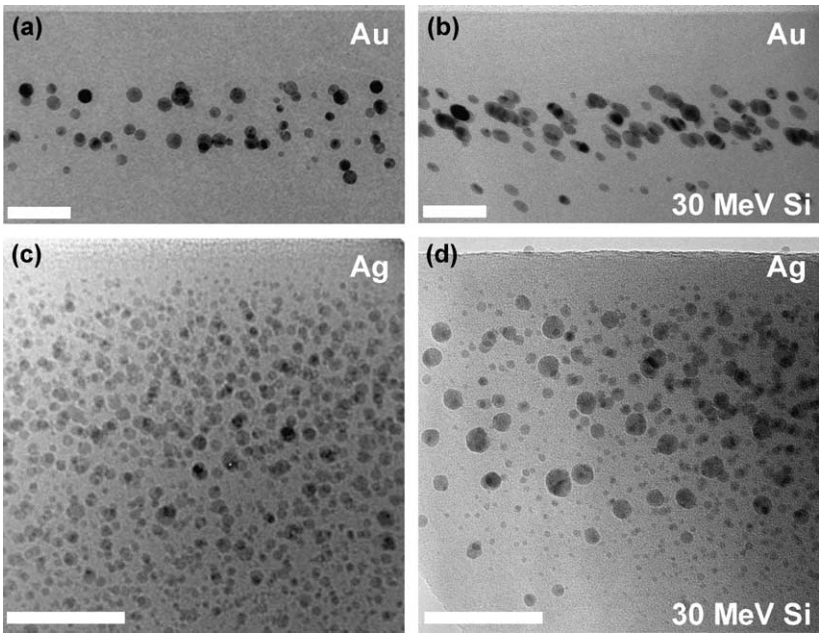

Fig. 3. Cross-section TEM images of (a) Au colloids in SiO_2 formed by Au ion implantation (peak concentration 1.6×10^{21} cm^{-3}) followed by thermal annealing at 1150 °C (1 h); (b) same as (a), after irradiation with 30 MeV Si (9.3×10^{14} cm^{-2}) at an angle of 60° off-normal; (c) Ag colloids in SiO_2 formed by Ag ion implantation (peak concentration 1.6×10^{21} cm^{-3}) followed by annealing at 500 °C (1 h); (d) same as (c), after irradiation with 30 MeV Si (9.3×10^{14} cm^{-2}) at an angle of 60° off-normal. Scale bars 50 nm.

4. Conclusions

Silica–Au core–shell colloids with a typical diameter of 400 nm show anisotropic plastic deformation under MeV ion irradiation, with the metal flowing conform the anisotropically deforming silica core. The 20-nm thick metal shell imposes a mechanical constraint on the deforming silica core, reducing the net deformation compared to that of pure silica. Adding an additional silica shell to these particles again enhances the deformation strain.

In Au–silica core–shell colloids, the silica expands perpendicular to the ion beam, while the metal core shows a large expansion along the ion beam direction, provided the silica shell thickness is large enough (>20 nm). By comparing experiments at different ion energies it is concluded that the metal deformation only occurs above an electronic energy loss threshold in the silica of ~3.3 keV/nm. Silver cores embedded in a silica shell do not show elongation, but rather disintegrate. Also in planar SiO_2 films, Au and Ag colloids show an entirely different behavior. We conclude the deformation model must include ion-induced particle disintegration in combination with thermodynamic effects, possibly in combination with mechanical effects driven by stresses around the ion tracks.

Acknowledgments

This work is part of the research program of the Foundation for Fundamental Research on Matter (FOM) and was financially supported by the Dutch Organization for Scientific Research (NWO). It was also supported by the EC Large Scale Facility in Rossendorf "AIM-Center for Application of Ion Beams in Materials Research", Project No. ERB FMGE CT98 0146. The Canadian part of this work was financially supported by NSERC, and FCAR. Bart Kooi (Materials Science Center, Groningen University) is gratefully acknowledged for TEM analysis in the early phase of this work, Frans Tichelaar (National Institute for high-resolution electron microscopy, Delft University) is gratefully acknowledged for TEM analysis in Section 3.2. We also happily acknowledge many stimulating discussions with Karl-Heinz Heinig (Research Center Rossendorf), Harry Bernas (CSNSM, Orsay) and Marcel Toulemonde (Caen).

References

[1] S. Klaumünzer, G. Schumacher, Phys. Rev. Lett. 51 (1983) 1987.
[2] H. Trinkaus, A.I. Ryazanov, Phys. Rev. Lett. 74 (1995) 5072.
[3] T. van Dillen, A. Polman, P.R. Onck, E. van der Giessen, Phys. Rev. B 71 (2005) 24103.
[4] E. Snoeks, A. van Blaaderen, C.M. van Kats, M.L. Brongersma, T. van Dillen, A. Polman, Adv. Mater. 12 (2000) 1511.
[5] S. Klaumünzer, Nucl. Instr. and Meth. B 215 (2004) 345.
[6] K.P. Velikov, T. van Dillen, A. Polman, A. van Blaaderen, Appl. Phys. Lett. 81 (2002) 838.
[7] D.L.J. Vossen, D. Fific, J.J. Penninkhof, T. van Dillen, A. Polman, A. van Blaaderen, Nano Lett. 5 (2005) 1175.
[8] M. Hou, S. Klaumünzer, G. Schumacher, Phys. Rev. B 41 (1990) 1144.
[9] S. Klaumünzer, Nucl. Instr. and Meth. B 225 (2004) 136.
[10] A. Audouard, E. Balanzat, S. Bouffard, J.C. Jousset, A. Chamberod, A. Dunlop, D. Lesueur, G. Fuchs, R. Spohr, J. Vetter, L. Thomé, Nucl. Instr. and Meth. B 59/60 (1991) 414.
[11] T. van Dillen, E. Snoeks, W. Fukarek, C.M. van Kats, K.P. Velikov, A. van Blaaderen, A. Polman, Nucl. Instr. and Meth. B 175 (2001) 350.

[12] Z.G. Wang, C. Dufour, E. Paumier, M. Toulemonde, J. Phys.: Condens. Matter 6 (1994) 6733.
[13] C. D'Orléans, J.P. Stoquert, C. Estournès, C. Cerruti, J.J. Grob, J.L. Guille, F. Haas, D. Muller, M. Richard-Plouet, Phys. Rev. B 67 (2003) 220101.
[14] C. D'Orléans, C. Cerruti, C. Estournès, J.J. Grob, J.L. Guille, F. Haas, D. Muller, M. Richard-Plouet, J.P. Stoquert, Nucl. Instr. and Meth. B 209 (2003) 316.
[15] C. D'Orléans, J.P. Stoquert, C. Estournès, J.J. Grob, D. Muller, J.L. Guille, M. Richard-Plouet, C. Cerruti, F. Haas, Nucl. Instr. and Meth. B 216 (2004) 372.
[16] C. D'Orléans, J.P. Stoquert, C. Estournès, J.J. Grob, D. Muller, C. Cerruti, F. Haas, Nucl. Instr. and Meth. B 225 (2004) 154.
[17] C. Graf, A. van Blaaderen, Langmuir 18 (2002) 524.
[18] W. Stöber, A. Fink, E. Bohn, J. Coll. Interf. Sci. 26 (1968) 62.
[19] C. Graf, D.L.J. Vossen, A. Imhof, A. van Blaaderen, Langmuir 19 (2003) 6693.
[20] A. Benyagoub, S. Klaumünzer, Radiat. Eff. Def. Sol. 126 (1993) 105.
[21] T. van Dillen, A. Polman, C.M. van Kats, A. van Blaaderen, Appl. Phys. Lett 83 (2003) 4315.
[22] C.A. Volkert, A. Polman, Mater. Res. Soc. Symp. Proc. 235 (1992) 3.
[23] E. Snoeks, K.S. Boutros, J. Barone, Appl. Phys. Lett. 71 (1997) 267.
[24] A. Benyagoub, A. Chamberod, J.C. Dran, A. Dunlop, F. Garrido, S. Klaumünzer, L. Thomé, Nucl. Instr. and Meth. B 106 (1995) 500.
[25] J.J. Penninkhof, T. van Dillen, A. Polman, C. Graf, A. van Blaaderen, Adv. Mater. 17 (2005) 1484.
[26] S. Roorda, T. van Dillen, A. Polman, C. Graf, A.M. Vredenberg, A. van Blaaderen, B. Kooi, Adv. Mater. 16 (2004) 235.
[27] J.F. Ziegler, J.P. Biersack, U. Littmark, The Stopping and Range of Ions in Solids, Pergamon, New York, 1985.
[28] M. Strobel, K.H. Heinig, W. Möller, Phys. Rev. B 64 (2001) 245422.
[29] E. Valentin, H. Bernas, C. Ricolleau, F. Creuzet, Phys. Rev. Lett. 86 (2001) 99.
[30] E. Snoeks, T. Weber, A. Cacciato, A. Polman, J. Appl. Phys. 78 (1995) 4723.
[31] A.M. Vredenberg, T. van Dillen, J.J. Penninkhof, M. Toulemonde, K.H. Heinig, P.R. Onck, E. van der Giessen, A. van Blaaderen, A. Polman, unpublished.